

## Analysis of Stiffened Granular Piled Raft

Madhav Madhira<sup>1</sup>, Jitendra Kumar Sharma<sup>2</sup> and Raksha Rani Sanadhya<sup>3</sup>

<sup>1</sup>Civil Engineering Dept., Jawaharlal Nehru Technological University, Hyderabad 500072, India

<sup>2</sup>Civil Engineering Dept., Rajasthan Technical University, University Department, Kota-324010, India

<sup>3</sup>Civil Engineering Dept., Government Polytechnic College, Kota-324010, India

<sup>1</sup>Email: madhavmr@gmail.com

<sup>2</sup>Email: jksharma@rtu.ac.in

<sup>3</sup>Email: rrsanadhya.phd14@rtu.ac.in

**ABSTRACT:** Piled rafts are usually provided to reduce total and differential settlements of foundation and structures built on deep deposits of soft or problematic soils. Granular piles may be used in place of conventional concrete or steel piles because of their several additional advantages. The load carrying capacity of these granular piles (GP) can be increased for improved performance by stiffening of granular piles their top portion of length by relatively strong material having better strength and stiffness, i.e. higher deformation modulus in comparison to the material of granular pile in the lower portion. Geogrid encased columns, SDCM (stiffened deep cement mixing), fibre reinforced granular columns, etc. are common forms of stiffening GP. The present study deals with the analysis of partially stiffened granular pile with rigid raft based on the continuum approach. The overall response of the top stiffened GP-raft foundation is evaluated in terms of settlement influence factor, settlement reduction factor in comparison to un-stiffened granular piled raft, normalized GP-soil interface shear stresses, percentage load shared by GP, normalized contact pressure distribution beneath the raft and percentage load transfer to the base of GP with relative stiffness factor and relative length of stiffening.

**KEYWORDS:** Granular piled raft, Stiffness factor, Relative stiffness of granular pile, Relative length of stiffening, Settlement influence factor

### 1. INTRODUCTION

Piled raft technique has been developed since nineteen eighties and used to reduce total and differential settlements as also the tilt of tall structures. This foundation system has been most notably applied to high-rise buildings all over the world and increasingly being recognized as an effective and economical system, for bridges and heavy industrial plants as well. Piled-raft system works through the combined action of the three bearing elements, viz., raft, piles and subsoil. Piles are mainly of reinforced concrete/steel and are very expensive to install. Stone columns/granular piles (GP), composed of compacted gravel, sand or mixture of both, can be used in place of concrete/steel. Due to higher demand for increase in load carrying capacity of granular pile, their strength and stiffness need to be increased. Bulging failure of granular pile is often the controlling mode. Maximum bulge in the pile was observed to be about one to two pile diameters from the ground surface (Bergado and Lam 1987). The load carrying capacity of granular piles can be increased and bulging avoided by (i) using concrete plug (ii) placing horizontal reinforcement at upper portion of granular pile (iii) using circumferential reinforcement with geogrid casing or jacket or (iv) mixing the granular material strength with fibres (Madhav et al., 1994). Stiffening means replacement of material in the top region of pile with higher value of deformation modulus. Geogrid encased columns, SDCM (stiffened deep cement mixing), fibre reinforced granular columns, etc. are common forms of stiffening of granular pile.

To predict the behavior of soft ground treated with columnar inclusion, various theoretical analyses have been proposed based on the "Unit Cell" concept (Baalam & Booker 1981, Van Impe & Madhav 1994, Alamgir 1996, Elshazly et al. 2008, Zhang et al. 2015). Piled raft systems were analyzed numerically, based on the boundary element method, the continuum approach and simplified stiffness approach (Butterfield & Banerjee 1971b, Polous 1968, Davis & Polous 1972, Randolph 1983).

Shahu et al. (2000) present a simple approach to analyze soft ground reinforced by granular pile with granular mat on the top. The response of piled raft foundation on soft soil strengthened by short granular piles made of flexible materials was investigated by Liang et al. (2003). Madhav et al. (2006) carried out settlement analysis of a granular pile considering non-homogeneities in the deformation modulus of the in situ soil as well as of granular pile material.

Madhav et al. (2009) investigated the interactions between a granular pile and raft using the continuum approach. Yamashita and Yamada (2009) and Yamashita et al. (2011) carried out the analysis of piled raft with grid-form deep cement mixes pile walls for seven and twelve story buildings on soft cohesive and liquefiable soil. Wang et al. (2010) brought out conceptual performance of composite piled raft foundation under vertical loading with stone columns, lime columns and steel pipe piles. Maheshwari and Khatri (2010, 2011) concluded that the performance in terms of deformation of combined footing on very soft soil can be improved by providing stone columns with a granular fill layer just below the footing.

Das and Deb (2014) developed a mechanical model to study the behaviour of uniformly loaded circular raft resting on stone column improved ground. Park et al. (2016) analyzed load sharing behavior of piled rafts installed with driven piles in sand. The effects of pile length and alignment on the attained ultimate load were investigated by Elwakil and Azzam (2016). El-garhy and Elsaywy (2017) presented a method to analyze strip footing resting on granular layer over weak soil improved by end bearing or floating granular piles. Grover and Sharma (2015) evaluated vertical displacements of stiffened granular pile, (its top portion replaced partially by relatively strong stiff material) based on continuum approach. Gupta and Sharma (2018) carried out settlement analysis of a non-homogeneous granular pile with non-linear variation of deformation modulus with depth.

Garg and Sharma (2018) developed analytical solutions based on elastic continuum approach to predict the settlement of partially stiffened single and group of two floating granular piles. Effect of nonlinear non-homogeneity of floating granular pile and soil on the settlement of a granular pile was presented by Gupta and Sharma (2018). They concluded that the reduction in the magnitude of settlement influence factor further increases depending on non-homogeneity parameters and with the increment in the relative length of pile ( $L/d$ ).

Present study deals with the analysis of partially stiffened granular pile with rigid raft based on the elastic continuum approach. The objectives of this study to include the effect of stiffening of upper portion of pile and relative length of stiffening on

- The settlement influence factor
- Settlement reduction factor in comparison to un-stiffened granular piled raft

- Settlement factor in comparison to partially stiffened single pile
- Normalized GP-soil interface shear stresses
- Percentage load shared by GP, base of GP and raft
- Normalized contact pressure distribution beneath the raft.

## 2. PROBLEM DEFINITION

Partially stiffened granular piled raft foundation carrying an axial load,  $P$ , with GP of length  $L$  and diameter,  $d=2a$ , is depicted in Figure 1. The soft soil is characterized by its modulus of deformation,  $E_s$ , and Poisson's ratio,  $\nu_s$ . The granular pile is compressible with modulus of deformation,  $E_{gp}$ . The relative stiffness of GP is defined as  $K_{gp}=E_{gp}/E_s$ , the ratio of deformation moduli of granular pile to that of the soil. In the present analysis it is assumed that top portion of length,  $L_s=\lambda L$  has been stiffened. The modulus of deformation of stiffened portion is  $E_{stgp}$ . Relative stiffness,  $\mu = K_{stgp}/K_{gp}$ , ratio of moduli of stiffened and un-stiffened portions of GP. The values of deformation modulus of GP are different in stiffened and un-stiffened portion but they are assumed same and uniform with the depth of GP in their respective regions. The values of  $\nu_{gp}$  can be taken different for stiffened and un-stiffened portion in analysis but Poisson ratio,  $\nu_{gp}$  is assumed same for both portions of the GP as it does not influence the result significantly. For numerical integration, the pile is discretized in to 'n' cylindrical elements and each element is further subdivided vertically into 'nz' and circumferentially in to 'nt' sub-element as shown in Figure 2.

assumed to be smooth and rigid and (iv) Stress strain relationships of soil and GP material are linear.

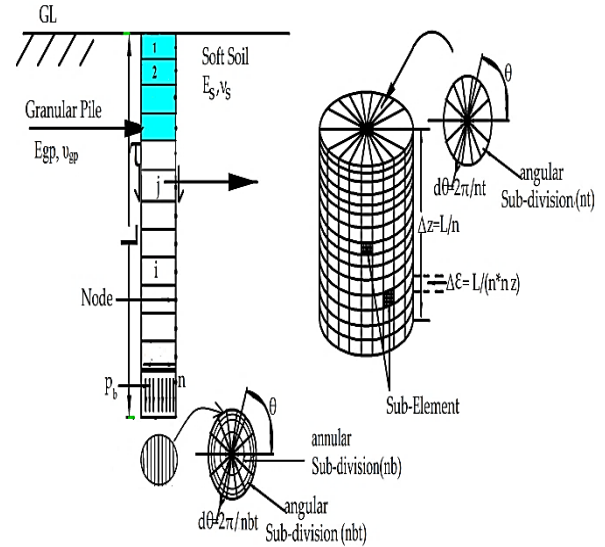
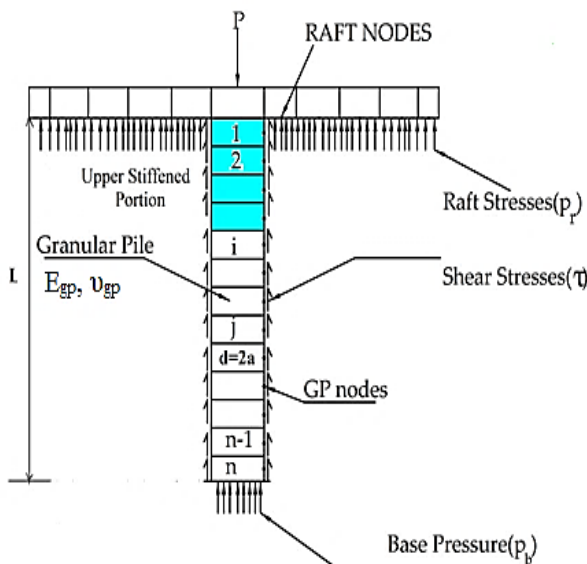


Figure 2 Pile discretization Scheme (after Sharma (1999))



### Figure 1 Force and Stresses on a Partially Stiffened Piled Raft Foundation

The raft is assumed to be rigid and of diameter,  $D$ . For numerical integration, raft is discretized into 'kr' number of annular rings of equal areas. It is further subdivided into 'kt' number of angular subdivisions as shown in Figure 3. ' $\tau$ ' are the interface shear stresses between GP and soil, ' $p_r$ ' the contact pressures at the raft-soil interface and ' $p_b$ ' is base pressure at the pile tip as shown in Figure 4. Settlement nodes are at the interfaces of soil and raft and at the GP-soil interface.

### 3. METHODOLOGY

Mindlin's(1936) and Boussinesq's solutions for a point load in the interior and on the surface of a semi-infinite elastic solid respectively are adopted. Following are the assumptions made in the analysis: (i) The soil is homogeneous, isotropic and linearly elastic, (ii) The sides of GP are perfectly rough with no slip, (iii) Granular pile base is

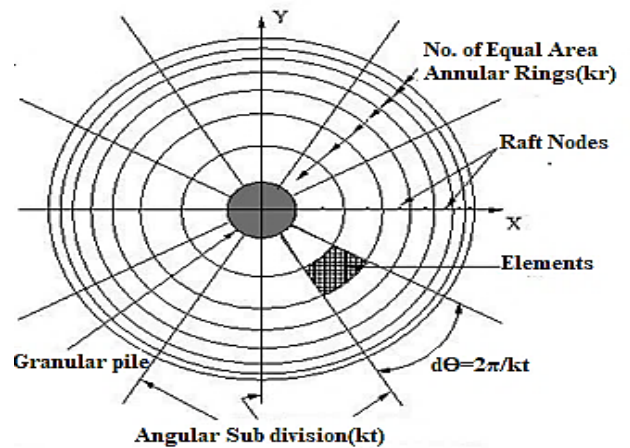


Figure 3 Raft discretization Scheme

### 3.1 Soil Displacements

Displacements along GP-soil interface are evaluated at the mid-point on the side of each element and at the centre of the base by integration of Mindlin & Boussinesq's expressions based on the influence of the elemental stresses of GP and the raft stresses respectively in matrix form following Sharma and Madhav (1999).

$$\left\{\rho^{\text{sp}}\right\}=\left\{\frac{S^{\text{sp}}}{d}\right\}=\left[I_{pp}\right]\left\{\frac{\tau}{E_s}\right\}+\left[I_{pr}\right]\left\{\frac{p_r}{E_s}\right\} \quad (1)$$

where  $\{\mathbf{S}^{\text{sp}}\}$  and  $\{\rho^{\text{sp}}\}$  are vertical and normalized vertical soil displacement vectors,  $[\mathbf{I}_{\text{pp}}]$ = square matrix of size  $(n+1)$  of the displacement influence coefficients evaluated by integrating Mindlin's equation (vertical displacements due to vertical point load within the semi-infinite elastic continuum) for the effect of GP elemental shear stresses and base pressure on settlements of nodes of pile elements,  $[\mathbf{I}_{\text{pr}}]$ = matrix of size  $(n+1) \times k_r$ , of the displacement

influence coefficients evaluated by integrating Boussinesq's equation (vertical displacements due to vertical point load at the surface) for the effect of raft stresses on settlements of nodes of pile elements and  $\{\tau\}$  and  $\{p_r\}$  - column vectors of sizes,  $\{n+1\}$  and  $\{kr\}$  respectively.

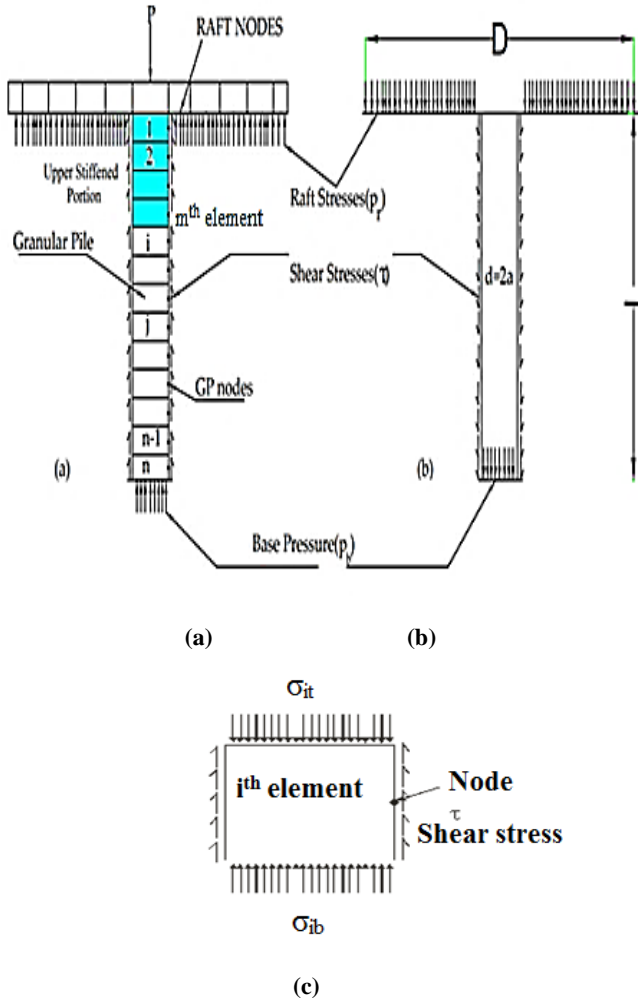


Figure 4 (a) Stresses on the GP and Raft due to Soil, (b) Stresses in the Soil due to GP and Raft and (c) Stresses on any  $i^{th}$  element of the GP

Displacements for soil-raft nodes are evaluated based on the interaction of elemental stresses from raft and GP. Soil displacement equations for raft nodes in matrix form are

$$\{\rho^{sr}\} = \left\{ \frac{S^{sr}}{d} \right\} = [I_{rp}] \left\{ \frac{\tau}{E_s} \right\} + [I_{rr}] \left\{ \frac{p_r}{E_s} \right\} \quad (2)$$

where  $\{S^{sr}\}$  and  $\{\rho^{sr}\}$  are vertical and normalized vertical soil displacement vector,  $[I_{rp}]$  = matrix of size,  $kr \times (n+1)$ , whose displacement influence coefficients are evaluated by integrating Mindlin's equation considering the effect of GP elemental shear stresses on settlement of raft nodes  $[I_{rr}]$  = square matrix of size 'kr' of the displacement influence coefficients evaluated by integrating Boussinesq's equation for the effect of raft stresses on the settlements of raft nodes and  $\{\tau\}$  and  $\{p_r\}$  - column vectors of size  $\{n+1\}$  and  $\{kr\}$  respectively.

### 3.2 Granular Pile Displacement

Formulation for the granular pile displacement is explain in appendix and described as per Equation (20A) of appendix. The vertical displacements of GP nodes in terms interface shear stresses are

$$\{\rho^{ppv}\} = \rho_t \{1\} + [C] \left\{ \frac{\tau}{E_s} \right\} \quad (3)$$

where  $[C]$  is a square matrix of size,  $(n+1) = [B] [A]$ .

### 3.3 Raft displacements

Raft is considered as rigid and hence displacements of raft nodes are all equal. Displacements of the top of the GP ( $\rho_t$ ) are all equal to raft displacement and expressed as

$$\{\rho^r\} = \rho_t \{1\} \quad (4)$$

where  $\{\rho^r\}$  is the raft displacement vector of size 'kr'.

### 3.4 Condition of Compatibility

- For satisfying the compatibility of displacements of the granular pile and the soil

$$\{\rho^{sp}\} = \{\rho^{ppv}\} \quad \text{or} \quad [AA] \left\{ \frac{\tau}{E_s} \right\} + [I_{pr}] \left\{ \frac{p_r}{E_s} \right\} = \rho_t \{1\} \quad (5)$$

where  $[AA] = [I_{pp}] - [C]$  of size  $(n+1) \times (n+1)$

- For compatibility of displacements of the raft and the soil

$$\{\rho^{sr}\} = \{\rho^r\} \quad \text{or} \quad [I_{rp}] \left\{ \frac{\tau}{E_s} \right\} + [I_{rr}] \left\{ \frac{p_r}{E_s} \right\} = \rho_t \{1\} \quad (6)$$

Solving the Equations (5) & (6), normalized raft stresses and normalised interfacial shear stresses are evaluated. The settlement at the top of partially stiffened GP-Raft foundation is evaluated as

$$S^P = \frac{P}{E_s d} I_p \quad (7)$$

where  $I_p$  is settlement influence factor. Under the axial load, 'P', on partially stiffened granular piled raft the settlement influence factor for any depth,  $I_{pd}$ , is defined as

$$S^P = \frac{P}{E_s d} I_{pd} \quad (8)$$

where  $I_{pd}$  is settlement influence factor of granular pile.

Results are evaluated and discussed in terms of following parameters to quantify the effect of stiffening the GP. Settlement factor,  $\alpha$ , is

$$\alpha = \frac{\text{settlement of stiffened piledraft}}{\text{settlement of stiffened pile alone}} \quad (9)$$

Settlement reduction factor,  $\beta$ , is

$$\beta = \frac{\text{settlement of stiffened pile raft}}{\text{settlement of unstiffened pile raft}} \quad (10)$$

The parameters defined above are for partially stiffened GP, i.e.,  $\mu > 1$ .  $\mu = 1$  corresponds to raft on un-stiffened GP.

#### 4. RESULTS AND DISCUSSION

Results obtained in this analysis have been validated first with those of continuum approach Poulos (1968), Randolph (1983) and Sharma and Madhav (2009) for rigid raft on a single compressible un-stiffened floating pile. The agreement has been very close (Table 1).

Table 1 Comparison of Settlements for Rigid- Piled Raft

Parameters	Load on Granular pile (%) ( $P_p/P$ ) $\times 100$	Ratio of Settlements of Piled raft to Pile alone ( $S_{pr}/S_p$ )	Reference
Floating Pile with raft $L/d=10, K_{gp}=\infty, v_s=0.5, D/d=3$	72	0.92	Continuum approach Poulos 1968
Floating Pile with raft $L/d=10, K_{gp}=\infty, v_s=0.5, D/d=3$	76	0.96	Approximate analysis Randolph 1983
Floating Pile with raft $L/d=10, K_{gp}=5000, v_s=0.5, D/d=3$	71.2	0.94	Sharma and Madhav 2009
Floating Pile with raft $L/d=10, K_{gp}=5000, v_s=0.5, D/d=3$	71.91	0.9213	Present Analysis

Results are obtained for the following ranges of non-dimensional parameters, relative length of GP,  $L/d = 10-40$ , relative stiffness,  $K_{gp}$  of GP = 10-1000, relative size of raft,  $D/d = 2-10$ , stiffness factor,  $\mu = 1-10$ , Poisson's ratio of soil,  $v_s = 0.3-0.5$ , Poisson's ratio of GP,  $v_{gp} = 0.3-0.5$  and relative length of stiffening from top of GP,  $\lambda = 0.1-0.4$ . Effect of Poisson's ratios of surrounding soil and granular pile do not affect the results significantly. Although the realistic range of  $K_{gp}$  for GP are 10-100, results are obtained for  $K_{gp} = 1000$ .

Figure 5 presents the variations of top settlement influence factor with the relative stiffness of GP for  $L/d=10$ , with relative length of stiffening from top of GP,  $\lambda=0.4$ , stiffness factor,  $\mu=1, 5$  and 10 and relative size of raft,  $D/d=3$  & 5. As expected, the settlement influence factor,  $I_p$ , decreases with the increase in the value of relative stiffness,  $K_{gp}$ . beyond  $K_{gp}=500$  there is not much significant change in the value of  $I_p$  with  $K_{gp}$  for both the value of  $D/d = 3$  and 5.

The settlement influence factor for single GP decreases from about 0.227 for homogeneous or un-stiffened GP ( $\mu=1$ ) at  $K_{gp}=10$ , and  $D/d=3$ , to about 0.194 and 0.185 for  $\mu$  equal to 5 and 10 respectively. The percentage reduction in the settlement influence factor,  $I_p$  from  $\mu=1$  to 5 is 14.5 and from  $\mu=1$  to 10 is 18.5. It is also observed that with the increase of stiffness factor,  $\mu$ , the value of settlement influence factor,  $I_p$ , decreases in the range of GP stiffness  $K_{gp}$  10 to 100 showing the effect of stiffening. This occurs due to the stiffer portion of GP transferring the stresses towards the lower portion and the base of the GP. The decrease in settlement influence factor,  $I_p$ , reduces with the increase in relative size of raft from  $D/d =$

3 to 5. For larger size of raft,  $D/d=5$  the values of settlement influence factor,  $I_p$ , is almost same for  $\mu=5$  and 10.

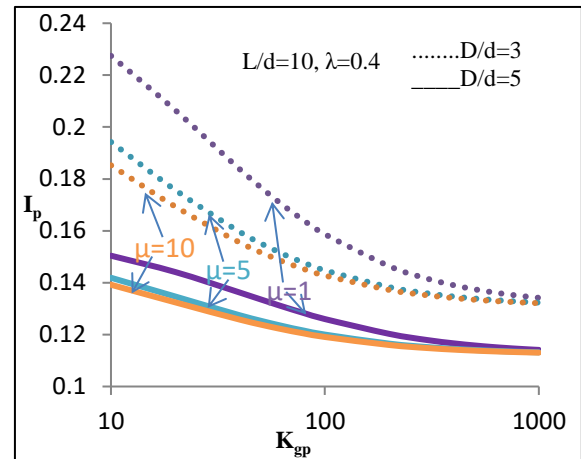


Figure 5 Variation of settlement influence factor,  $I_p$  with relative stiffness,  $K_{gp}$  of GP – effect of stiffness factor,  $\mu$ , and relative size of raft,  $D/d$ , on a partially stiffened GP-raft foundation ( $L/d=10, \lambda=0.4$ )

The influence of relative length,  $L/d$ , of GP, on the variation of settlement influence factor,  $I_p$ , with relative stiffness of GP,  $K_{gp}$ , is depicted in Figure 6 for  $\mu = 1, 5$  and 10. The settlement influence factor decreases with the increase of stiffness factor,  $\mu$ . For  $L/d = 10$   $I_p$  decreases from 0.226 to 0.185 for  $\mu$  increasing from 1 to 10. The values of  $I_p$  for  $K_{gp} = 10, \mu=5$  and  $L/d=10, 20$  and 40 are 0.194, 0.175 and 0.166 respectively. The percentage decreases in settlement influence factor,  $I_p$ , are 10 and 5.14 for increases in  $L/d$  from 10 to 20 and from 20 to 40 respectively. The rate of decrease of settlement influence factor,  $I_p$ , decreases with  $K_{gp}$ , and with increase in relative length,  $L/d$ . Settlement influence factor,  $I_p$ , is almost the same for the relative length,  $L/d$  increasing from 20 and 40 and for  $K_{gp} = 1000$ .

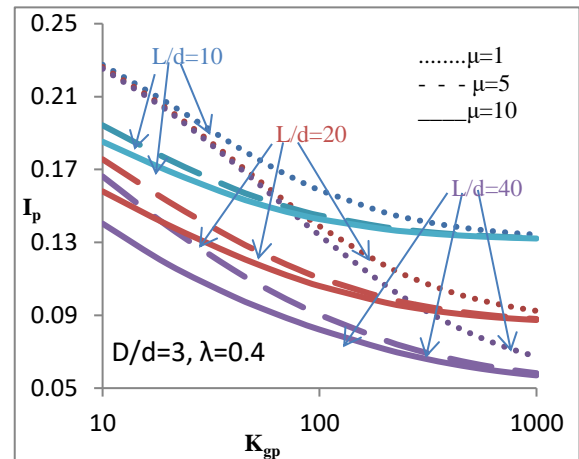


Figure 6 Variation of settlement influence factor,  $I_p$ , with relative stiffness,  $K_{gp}$ , of GP, - effect of relative length,  $L/d$ , of GP, and stiffness factor,  $\mu$ , on homogeneous GP-raft and partially stiffened GP-raft foundation ( $D/d=3, \lambda=0.4$ )

The variation of settlement influence factor,  $I_p$ , with relative stiffness,  $K_{gp}$ , of GP with the effect of relative length,  $\lambda$ , of stiffening from top of GP, for  $L/d = 10, \mu = 10$  and  $D/d=3$  and 5 is shown in Figure 7. The settlement influence factor,  $I_p$ , decreases with increase of relative stiffness,  $K_{gp}$ , of GP. The settlement influence factor,  $I_p$ , decreases with increase in the length of stiffening,  $\lambda$ , from top of GP. Values of  $I_p$  for  $D/d = 3, K_{gp} = 10$  and  $\lambda = 0.2, 0.3$  and 0.4 are 0.207,

0.195 and 0.185 respectively corresponding to percentage decreases of 5.8 and 10.6 due to the stiffening of the top portion. Influence factor  $I_p$ , is almost constant for  $K_{gp} \geq 100$ .

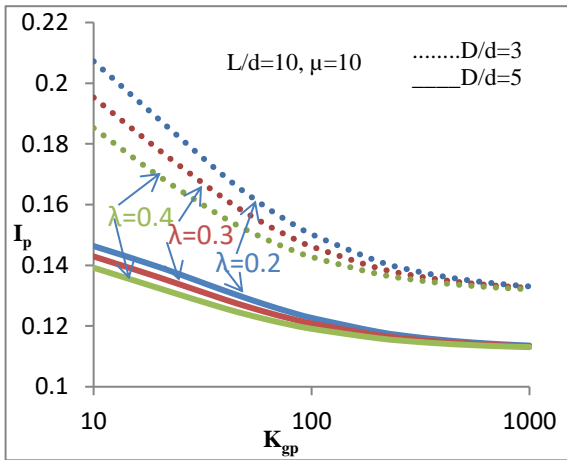


Figure 7 Variation of settlement influence factor,  $I_p$ , with relative stiffness,  $K_{gp}$  of GP – effect of relative length,  $\lambda$  of stiffening from top of GP, and relative size of raft,  $D/d$ , on partially stiffened GP-raft foundation ( $L/d=10$ ,  $\mu=10$ )

Figure 8 depicted the variation of settlement influence factor,  $I_p$ , with relative length of stiffening,  $\lambda$  from top of GP, with the effect of relative stiffness,  $K_{gp}$ , of GP, and relative size of raft,  $D/d$ . The settlement influence factor,  $I_p$ , decreases with increase of relative stiffness,  $K_{gp}$ , of GP, as well as with relative length,  $\lambda$  of stiffening from top of GP. For  $L/d = 10$ ,  $K_{gp} = 10$ ,  $D/d = 3$  for relative length of stiffening,  $\lambda$ , from top of GP, increasing from 0.1 to 0.4 settlement influence factor,  $I_p$ , decreases from 0.218 to 0.185, a decrease of about 15 percent. It can also be seen that stiffer piles ( $K_{gp} > 100$ ) are not much influenced with the increase in relative length of stiffening,  $\lambda$ .

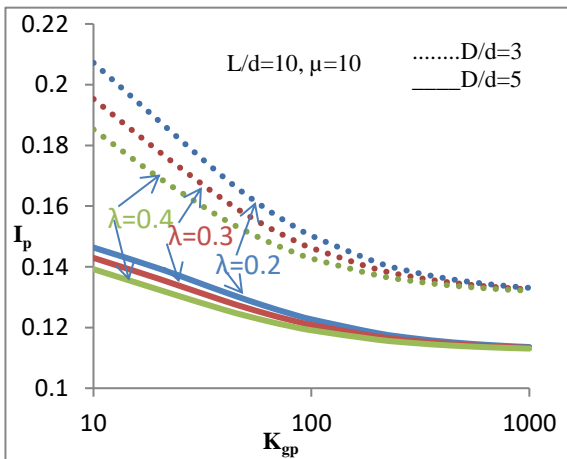


Figure 8 Variation of Variation of settlement influence factor,  $I_p$ , with relative stiffness of GP,  $K_{gp}$  – effect of relative length,  $\lambda$  of stiffening from top of GP, and relative size of raft,  $D/d$ , on partially stiffened GP-raft foundation ( $L/d=10$ ,  $\mu=10$ )

Figure 9 presented the variation of settlement influence factor,  $I_{pd}$ , of a GP with normalized depth,  $z_1=z/L$  for un-stiffened and stiffened granular piles with raft for  $L/d=10$ ,  $K_{gp}=100$ ,  $D/d=3$  and  $\lambda=0.4$ . Compatibility displacement at the interface of stiffened and un-stiffened portions of the GP is well satisfied. As stiffness factor,  $\mu$ , changes from un-stiffened condition of GP i.e. with,  $\mu=1$  to stiffened condition with,  $\mu=2$ , 5 and 10, the settlement influence factor,  $I_{pd}$ , for

top are respectively 0.154, 0.148, 0.143 and 0.142. The percentage decrease of settlement is 3.89, 7.14 and 7.79 respectively, showing the effect of stiffening. The rate of decrease of settlement influence factor decreases with increase in the stiffening of pile at the top.

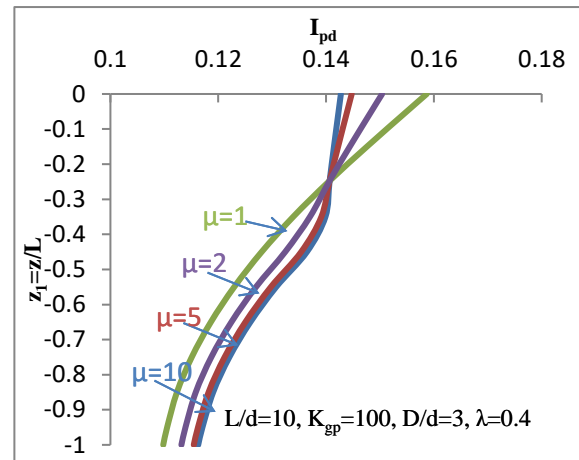


Figure 9 Variation of settlement influence factor for any depth,  $I_{pd}$ , with normalized depth,  $z_1=z/L$  – effect of stiffness factor,  $\mu$ , on homogeneous GP-raft and partially stiffened GP-raft ( $L/d=10$ ,  $K_{gp}=100$ ,  $D/d=3$ ,  $\lambda=0.4$ )

The variation of settlement influence factor,  $I_{pd}$ , of a GP with normalized depth,  $z_1 = z/L$ , is shown in Figure 10 with the effect of relative length  $\lambda$ , of stiffening from top of GP, for  $L/d=10$ ,  $K_{gp}=100$  and  $\mu = 2$ . For relative length of stiffening from top of GP,  $\lambda = 0.1$ , 0.2, 0.3 and 0.4 the values of settlement influence factor,  $I_{pd}$ , for top are respectively 0.154, 0.152, 0.150 and 0.148 for percentage decreases of 1.3, 2.6 and 3.9 respectively. Settlement influence factor,  $I_{pd}$ , decreases rapidly with depth in the lower region i.e. in un-stiffened portion of GP. For higher value of  $\lambda$  the value of  $I_{pd}$ , is maximum due to stresses transferred to the base with the length of stiffening.

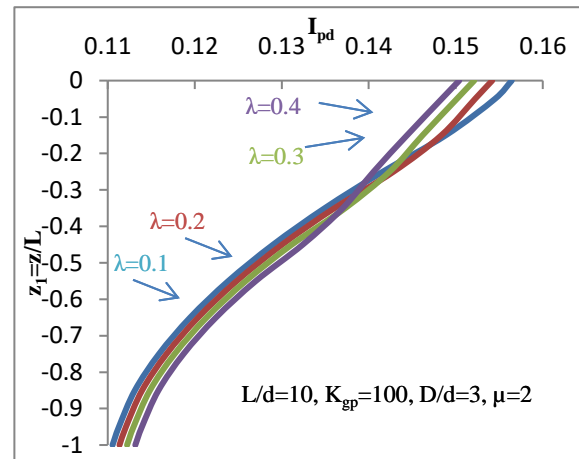


Figure 10 Variation of settlement influence factor for any depth,  $I_{pd}$ , with normalized depth,  $z_1=z/L$  – effect of relative length  $\lambda$ , of stiffening from top of GP, on partially stiffened GP-raft foundation ( $L/d=10$ ,  $K_{gp}=100$ ,  $D/d=3$ ,  $\mu=2$ )

Figure 11 depicted the variation of settlement reduction factor,  $\beta$ , with relative stiffness  $K_{gp}$ , of GP with the effect of stiffness factor,  $\mu$  for  $L/d=10$ ,  $D/d=3$ , and  $\lambda=0.2$  and 0.4.  $\beta$  is defined as ratio of settlement influence factor of stiffened part of the pile to that of un-stiffened pile and so it decreases with increasing stiffening of the upper portion of granular pile. The settlement reduction factor,  $\beta$



increases also with relative stiffness  $K_{gp}$ , of GP. The values of,  $\beta$  at,  $K_{gp}=10$ ,  $\lambda = 0.4$  and  $D/d = 3$  is about 0.932 for  $\mu=2$  and the corresponding values for  $\mu=5$  & 10 are 0.854 and 0.814 with percentage decreases of 8.36 and 1.52 for increases in  $\mu$  from 2 to 5 and from 5 to 10 respectively. All the values of  $\beta$ , converge to a single value at  $K_{gp}=1000$  since the granular pile is already very stiff and further increase in stiffening does not cause any change in values of  $\beta$ .

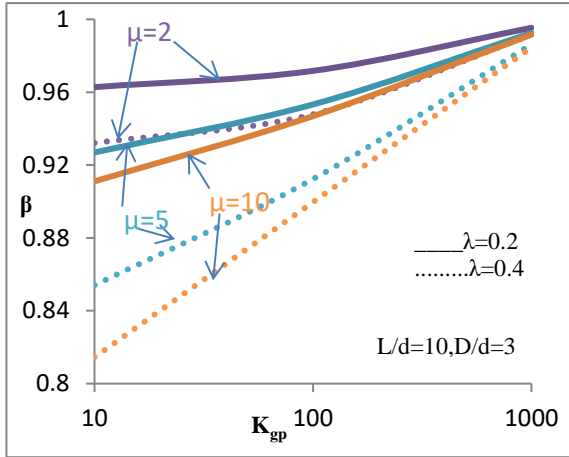


Figure 11 Variation of settlement reduction factor,  $\beta$ , with relative stiffness,  $K_{gp}$ , of GP –effect of stiffness factor,  $\mu$ , and relative length  $\lambda$ , of stiffening from top of GP, on partially stiffened GP-raft foundation ( $L/d=10, D/d=3$ )

From Figure 12 the value of settlement reduction factor,  $\beta$ , can be seen to decrease with increase in stiffness factor,  $\mu$ , revealing that the value of settlement for the partially stiffened piled raft decreases more than the value of settlement for un-stiffened piled raft. Settlement reduction factor,  $\beta$ , decreases with increase relative length of GP,  $L/d$ . The values of  $\beta$ , for  $K_{gp} = 100$ ,  $D/d=3$ ,  $\lambda = 0.4$ ,  $\mu=5$  and  $L/d=10, 20$  and 40 are 0.91, 0.79 and 0.67 respectively. The percentage decrease in settlement reduction factor,  $\beta$ , are 13 and 15 for increase in  $L/d$  from 10 to 20 and from 20 to 40 respectively.

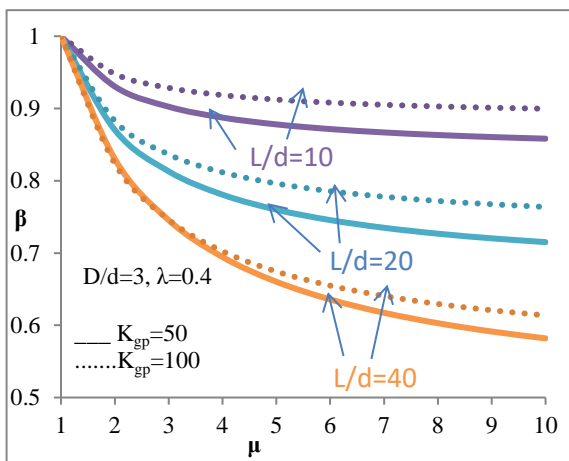


Figure 12 Variation of settlement reduction factor,  $\beta$ , with stiffness factor,  $\mu$ , –effect of relative length of GP,  $L/d$ , and relative stiffness of GP,  $K_{gp}$ , on partially stiffened GP-raft foundation ( $D/d=3, \lambda=0.4$ )

The variation of settlement reduction factor,  $\beta$ , with relative stiffness factor,  $\mu$ , with effect of relative size of raft,  $D/d$ , and relative stiffness  $K_{gp}$ , of GP is depicted in Figure 13. The settlement reduction factor,  $\beta$ , decreases with increase in the relative stiffness factor,  $\mu$ . The value of  $\beta$  for  $L/d = 10$ ,  $D/d=3$  and  $\lambda = 0.2$  and  $K_{gp} = 50$ , decreases

from 1 (for un-stiffened GP with  $\mu = 1$ ) to 0.962, 0.948 and 0.940 for  $\mu = 2, 3$  and 4 respectively.

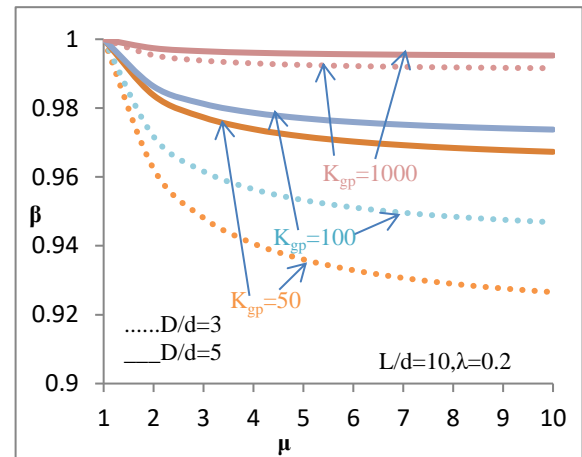


Figure 13 Variation of settlement reduction factor,  $\beta$  with stiffness factor,  $\mu$ , –effect of relative stiffness,  $K_{gp}$  of GP and relative size of raft,  $D/d$ , on partially stiffened GP-raft foundation ( $L/d=10, \lambda=0.2$ )

Figure 14 depicted the variation of settlement factor,  $\alpha$ , with the stiffness factor,  $\mu$ , with the effect of relative stiffness  $K_{gp}$ , of GP, and relative length,  $\lambda$  of stiffening from top of GP. The settlement factor,  $\alpha$ , increase with relative stiffness,  $K_{gp}$ , of GP implying that the settlement of stiffened pile alone is more than the settlement of stiffened piled raft. Since settlement factor,  $\alpha$ , also increases with increase in stiffness factor,  $\mu$ , and this effect is more for  $\mu$  in the range of 1-3. For the relative length of stiffening from top of GP,  $\lambda = 0.2$  the settlement factor,  $\alpha$ , converges to the same value at  $\mu = 10$  indicating that the effect of stiffening for shorter length of stiffening is less prominent than at higher values of stiffness factor from  $\mu = 6$ .

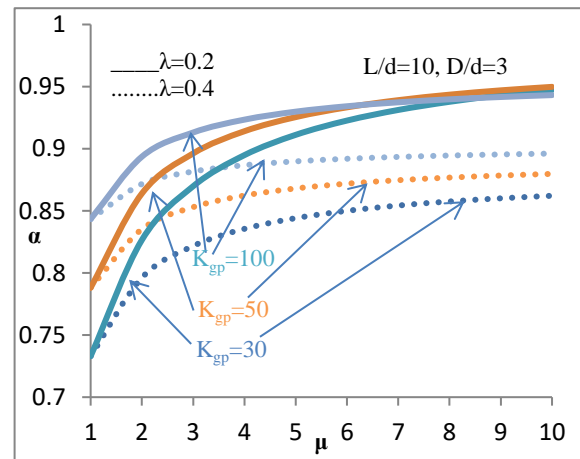


Figure 14 Variation of settlement factor,  $\alpha$ , with the stiffness factor,  $\mu$  – effect of relative stiffness  $K_{gp}$ , of GP, and relative length,  $\lambda$ , of stiffening from top of GP on partially stiffened GP-raft foundation ( $L/d=10, D/d=3$ )

Figure 15 depicted the variation of settlement factor,  $\alpha$  with stiffness factor,  $\mu$ , with the effect of relative length of GP,  $L/d$  for  $K_{gp}= 50$  and 100. With the increase in relative length,  $L/d$  of GP, the settlement factor,  $\alpha$ , increases because with increasing  $L/d$  there would be decrease in settlement influence factor for single pile as compare to that of piled raft. Similar trend is observed for  $K_{gp}= 50$  except that the settlement factor,  $\alpha$ , is less than that for  $K_{gp}= 100$ .

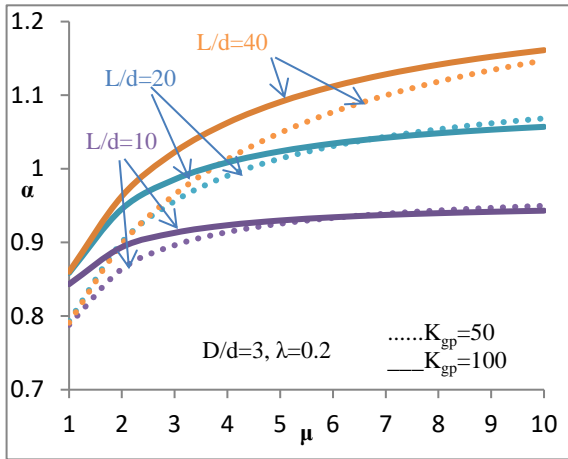


Figure 15 Variation of settlement factor,  $\alpha$ , with the stiffness factor,  $\mu$ , – effect of relative length of GP,  $L/d$ , and relative stiffness  $K_{gp}$ , of GP, on partially stiffened GP-raft foundation ( $D/d=3$ ,  $\lambda=0.2$ )

Figure 16 represents the variation of normalized shear stresses,  $\tau = \tau(\pi d L)/P$ , with the normalized depth,  $z_1 = z/L$  along with influence of relative length of stiffening from top of GP, for  $L/d=10$ ,  $K_{gp} = 50$  and 100,  $\mu=5$  and  $\lambda=0.2, 0.3$  and 0.4. Shear stresses decrease with increase of relative stiffness of GP,  $K_{gp}$ , but increase with the relative length of stiffening. The effect of increasing the length of stiffening from top of GP,  $\lambda$ , is to increase the shear stress towards the base of the GP.

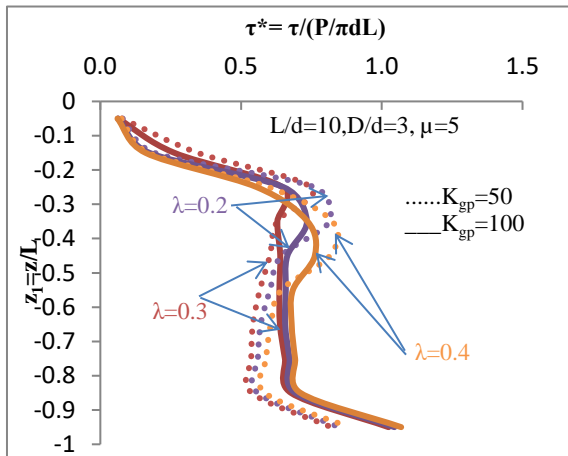


Figure 16 Variation of normalized shear stresses,  $\tau = \tau(\pi d L)/P$ , with the normalized depth,  $z_1 = z/L$  – effect of relative length of stiffening factor,  $\lambda$ , and relative stiffness of GP,  $K_{gp}$ , on a partially stiffened GP-raft foundation ( $L/d=10$ ,  $D/d=3$ ,  $\mu=5$ )

Figure 17 presents the variation of normalized shear stresses,  $\tau = \tau(\pi d L)/P$ , with normalized depth of pile  $z^* = z/L$  for  $L/d=10$ ,  $\lambda=0.4$ ,  $D/d=3$ ,  $K_{gp}=50, 100$  and for stiffness factor  $\mu = 1, 5$  and 10. Shear stresses increase throughout the length of granular pile with increase in stiffness factor,  $\mu$ . Shear stresses decrease over the stiffened portion and increases in un-stiffened portion of the granular pile.

The contact pressure distribution at the raft soil interface,  $P_r^* (P_r = (\pi d^2/4)/P)$ , with normalized distance from the center of raft,  $R^* = r/d$  can be seen in Figure 18, for  $L/d=10$ ,  $K_{gp}=50$ ,  $D/d = 3$  and 5 and  $\lambda=0.4$ . The percentage reduction in contact pressure for  $D/d = 3$  and 5 for  $\mu=5$  and 10 in comparison to the values for a homogeneous granular pile ( $\mu=1$ ) are 28% and 36% near the pile and 23% and 26.5% at the edge of pile respectively. For smaller size ( $D/d=3$ ) of raft, the stresses are about 54.6% lower than those for the larger size ( $D/d=5$ ) at the

edge of raft for  $\mu=10$ . The magnitude of normal stresses on raft decreases with increase in the stiffness of top portion of GP.

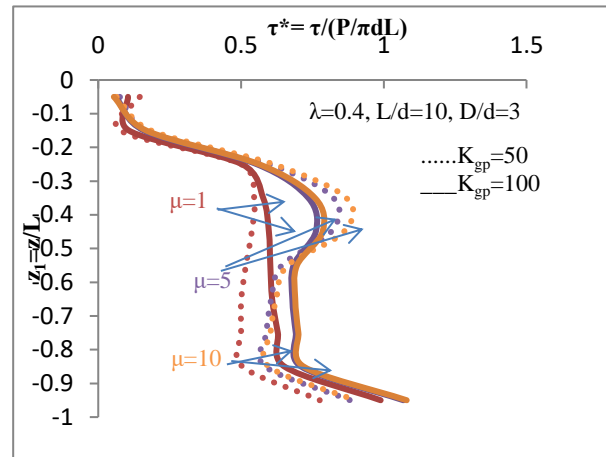


Figure 17 Variation of normalized shear stresses,  $\tau^* = \tau(\pi d L)/P$ , with the normalized depth,  $z_1 = z/L$  – effect of stiffness factor,  $\mu$  and relative stiffness,  $K_{gp}$ , of GP, on a partially stiffened GP-raft foundation ( $L/d=10$ ,  $D/d=3$ ,  $\lambda=0.4$ )

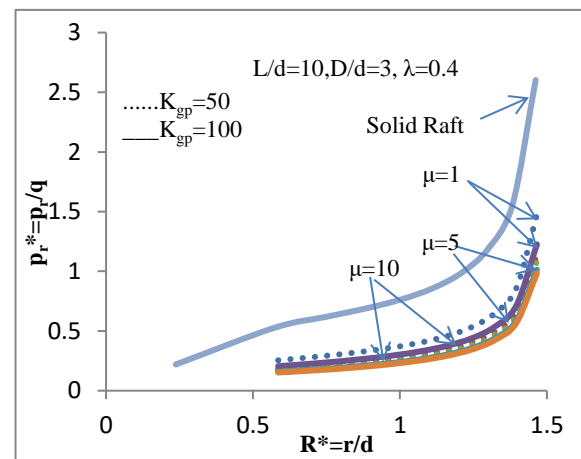


Figure 18 Variation of contact pressure ( $p_r^* = p_r/q$ ), with normalized distance from the center of raft  $R^* = r/d$ , – effect of stiffness factor,  $\mu$ , and relative size of raft,  $D/d$ , on partially stiffened GP-raft foundation ( $L/d=10$ ,  $K_{gp}=50$ ,  $\lambda=0.4$ )

Variations of contact pressures  $p_r^* = (P_r/q)$ , with normalized distance from the center of raft  $R^* = r/d$ , with stiffness factor,  $\mu$ , and relative stiffness,  $K_{gp}$ , of GP on a stiffened GP raft and raft alone are depicted in Figure 19. The contact pressure distribution pattern for partially stiffened raft is very similar to that of the raft alone with the normal stress beneath a rigid raft increasing with distance from the center and tending to very high values at the edge of the raft. The percentage reductions in the contact pressure for  $L/d=10$ ,  $D/d=3$ ,  $\mu = 10$  and  $K_{gp} = 50$  and 100 in comparison to the value for a solid raft are respectively 58.5% and 62.3% near the edge of raft. Contact pressure reduces with increase in relative stiffness,  $K_{gp}$  and relative stiffness factor,  $\mu$ .

Figure 20 shows the variation of percentage load ( $P_p/P$ ) transferred to the pile with relative stiffness,  $K_{gp}$ , of GP showing the influence of stiffness factor,  $\mu$ , for  $L/d=10$ ,  $\lambda=0.4$ . The percentage load shared by pile for  $K_{gp} = 10$ ,  $D/d = 3$  and  $\mu = 1, 5$  and 10 are 24.46, 45.23 and 50.87 respectively implying that the percentage pile load increases with the increase in stiffness factor,  $\mu$ . Pile load also increases with the increase of relative stiffness,  $K_{gp}$ , of GP.

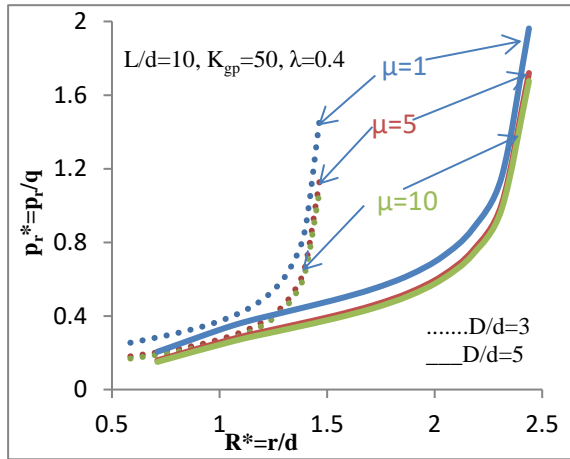


Figure 19 Variation of contact pressure ( $p_r^* = p_r/q$ ), with normalized distance from the center of raft  $R^* = r/d$ , –Effect of stiffness factor,  $\mu$ , and relative stiffness  $K_{gp}$ , of GP, on a partially stiffened GP-raft and solid raft ( $L/d=10$ ,  $D/d=3$ ,  $\lambda=0.4$ )

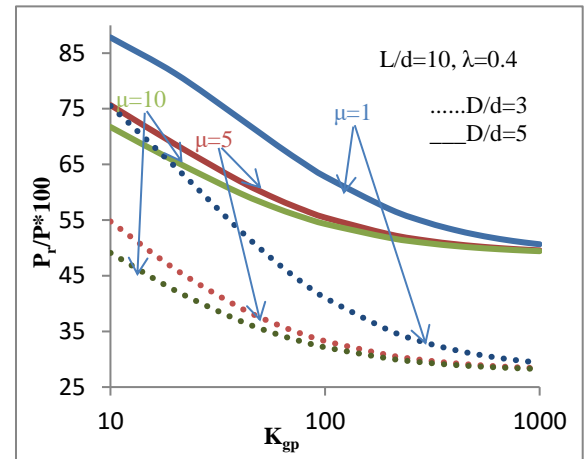


Figure 21 Variation of percentage load transferred to raft,  $(P_r/P) \times 100$ , with relative stiffness  $K_{gp}$ —effect of stiffness factor,  $\mu$ , and relative size of raft,  $D/d$  on partially stiffened GP-raft foundation ( $L/d=10, \lambda=0.4$ )

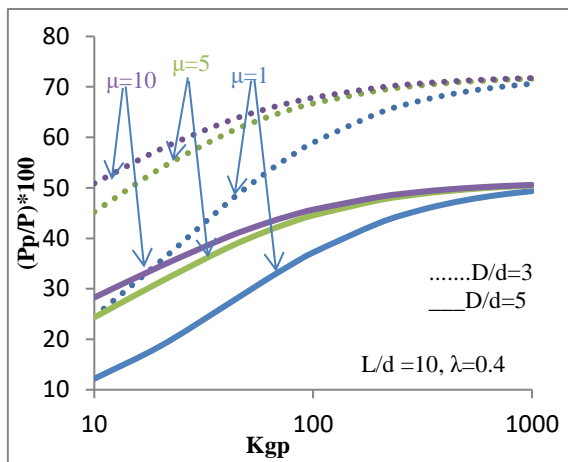


Figure 20 Variation of percentage pile load,  $(P_p/P) \times 100$ , with the relative stiffness,  $K_{gp}$ — effect of stiffness factor,  $\mu$ , and relative size of raft,  $D/d$ , on partially stiffened GP-raft foundation ( $L/d=10$ ,  $\lambda=0.4$ )

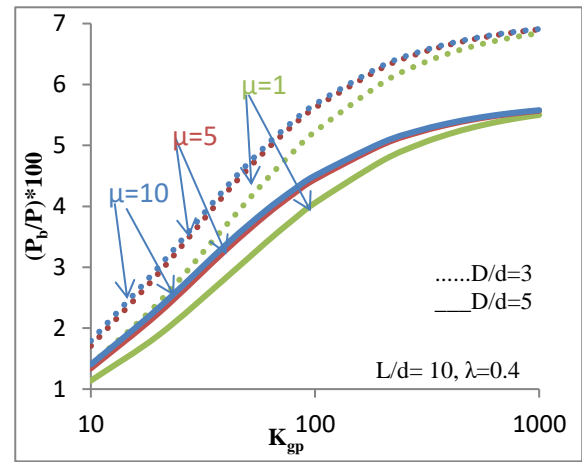


Figure 22 Variation of percentage Base load,  $(P_b/P) \times 100$ , with the relative stiffness,  $K_{gp}$  of GP— effect of stiffness factor,  $\mu$ , and relative size of raft,  $D/d$ , on partially stiffened GP-raft foundation ( $L/d=10, \lambda=0.4$ )

The variation of percentage load transferred to the raft,  $(P_r/P) \times 100$ , with relative stiffness of GP,  $K_{gp}$ , is depicted in Figure 21 with effect of stiffness factor,  $\mu$ , and relative size of raft,  $D/d$ , on a partially stiffened GP-raft for  $L/d = 10$  and  $\lambda = 0.4$ . For  $\mu = 5$  the percentage load carried by the raft increases from 55 to 75 for increase in raft size,  $D/d$ , from 3 to 5.

The variation of percentage base load  $(P_b/P) \times 100$  with relative stiffness,  $K_{gp}$ , can be seen in Figure 22 showing the influence of stiffness factor,  $\mu$  for  $L/d=10, \lambda=0.4$ . The percentage load transferred to the base of the piled raft increases with the increase in relative stiffness of GP,  $K_{gp}$ . Similarly, the percentage load transferred to the base,  $(P_b/P) \times 100$ , increases with increase of stiffness factor,  $\mu$ , showing the positive effect of stiffening. The percentage load carried by the base of GP decreases with the increase in relative size of raft,  $D/d$ .

Figure 23 depicts the variation of percentage load transferred to the base,  $(P_b/P) \times 100$ , with relative stiffness,  $K_{gp}$ , with the influence of relative length of stiffening from top of GP,  $\lambda$ , and relative size of raft,  $D/d$ , on a partially stiffened granular piled raft for,  $L/d=10$  and  $\lambda=0.4$ . The percentage base load increases with the increase in relative stiffness factor,  $K_{gp}$ , and relative length of stiffening from top of GP,  $\lambda$ . For  $\mu = 10$ ,  $L/d = 10$ ,  $K_{gp} = 10$  and  $\lambda = 0.2, 0.3$  and  $0.4$  the values of percentage base loads are 1.54, 1.65 and 1.79 respectively.

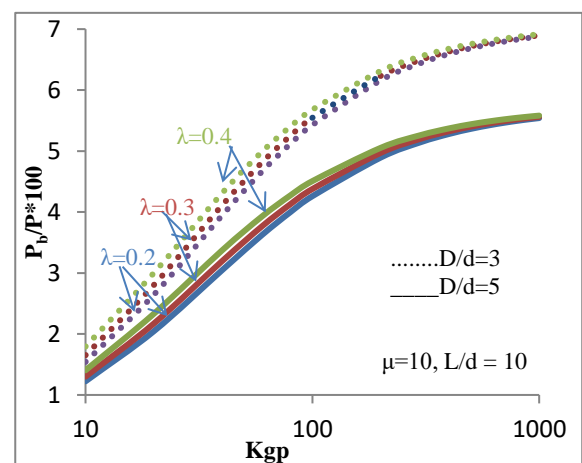


Figure 23 Variation of percentage base load,  $(P_b/P) \times 100$ , with the relative stiffness,  $K_{gp}$ , of GP – effect of relative length,  $\lambda$ , of stiffening from top of GP, and relative size of raft,  $D/d$ , on partially stiffened GP-raft foundation ( $L/d=10, \mu=10$ )



Figure 24 depicts the variation of percentage load transferred to the base,  $(P_b/P_p) \times 100$ , with relative stiffness,  $K_{gp}$ , with the influence of stiffness factor,  $\mu$ , and relative size of raft,  $D/d$  on a partially stiffened GP-raft for  $L/d=10$  and  $\lambda=0.4$ . As can be expected, the percentage load transferred to the base of GP increases with the increase of relative stiffness of GP,  $K_{gp}$ . The load transferred to the base decreases with the increase in stiffening factor,  $\mu$ , and with the increase of relative size of raft,  $D/d$ .

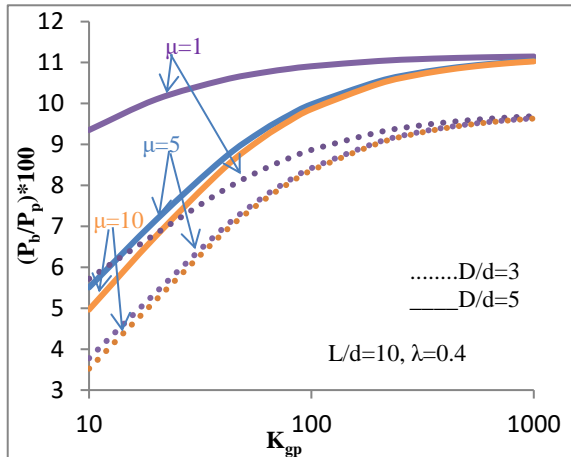


Figure 24 Variation of percentage load transferred to the base,  $(P_b/P_p) \times 100$ , with relative stiffness,  $K_{gp}$ , of GP –effect of stiffness factor,  $\mu$ , and relative size of raft,  $D/d$  on partially stiffened GP-raft foundation ( $L/d=10, \lambda=0.4$ )

## 5. CONCLUSION

Analysis of partially stiffened granular piled raft is presented based on elastic continuum approach in the current study. The following conclusions are drawn:

- The settlement influence factor  $I_p$  and  $\beta$  decrease with increase in stiffness factor. Decrease in the settlement influence,  $I_p$  is about 14% for  $\mu$  increasing from 1 to 5 and only 4% from  $\mu$  increasing from 5 to 10 for  $L/d=10$ ,  $K_{gp} = 10$ ,  $D/d = 3$  and  $\lambda = 0.4$  implying that the effect of  $\mu$  is more pronounced in the smaller range of stiffness factor  $\mu=1-5$ . Further stiffening of granular pile in the top portion does not make significant change in the settlement reduction.
- Settlement influence factor,  $I_p$ , for partially stiffened granular piled raft reduces with the increase in relative length of stiffening from top of GP,  $\lambda$ . Percentage reduction in settlement influence factor is approximately 10% for relative length of stiffening,  $\lambda$ , increasing from 0.2 to 0.4 for  $K_{gp}=10$ ,  $\mu = 10$ ,  $D/d=3$  and  $L/d=10$ . Thus effect of length of stiffening on settlement reduction is significant up to five times the diameter of GP.
- The settlement reduction factor,  $\beta$ , reduces with increasing stiffening parameters,  $\mu$  and  $\lambda$ . Reduction is about 15% with stiffness factor,  $\mu$ , increasing from 1 to 10 for  $K_{gp}=50$ ,  $L/d=10$ ,  $D/d=3$  and  $\lambda=0.4$ . For the same parameters the value of settlement reduction factor,  $\beta$ , reduces by about 29% for  $L/d = 20$ .
- The settlement factor,  $\alpha$ , increases by 24% for the stiffness factor,  $\mu$ , increasing from 1 to 5 for  $K_{gp}=30$ ,  $L/d=10$ ,  $D/d=3$ ,  $\lambda=0.2$  and about 28% for stiffness factor,  $\mu$ , increasing from 1 to 10. Stiffening is significant in the range of stiffness factor from 1 to 5.
- Normalized shear stresses for partially stiffened granular piled raft reduce about 48% at the top of the GP, due to stiffening for the stiffness factor,  $\mu$ , increasing from 1 to 5 for  $\lambda=0.4$ ,  $K_{gp}=50$ ,  $L/d=10$ , and  $D/d=3$ .

- The percentage reduction in the contact pressure at the raft soil interface in comparison to the value of a raft alone is 62.3% near the edge of raft for  $L/d = 10$ ,  $D/d = 3$ ,  $\mu = 10$  and  $K_{gp} = 100$ .
- The percentage load transferred to the base of GP increases with the increase stiffness factor and relative length of stiffening from top of GP and decreases with the increase relative size of raft.
- The percentage load transferred to the pile increases with the increase in stiffness parameters and relative stiffness of GP,  $K_{gp}$ .

## 6. REFERENCES

- Alamgir, M., Miura, N., and Madhav, M. R., (1994) "Analysis of granular column reinforced ground stress transfer from granular column to soil", Reports of the Faculty of Science and Engineering, Saga University, Saga, Japan, 23, 81-94.
- Alamgir, M., Muira, N., Poorooshasb, H. B., and Madhav, M. R., (1996) "Deformation analysis of soft ground reinforced by columnar inclusions" *Comput. and Geotech.*, 18(4), 267-290.
- Balaam, N.P., and Booker, J.R., (1981) "Analysis of rigid rafts supported by granular piles", *International Journal for Numerical and Analytical methods in Geomechanics*, 5, 379-403.
- Bergado, D.T., and Lam, F.L., (1987) "Full scale load test of granular piles with different densities and different proportions of gravel and sand in the soft Bangkok clay", *Soils & Foundations*, 27, 86-93.
- Butterfield, R. and Banerjee, P.K., (1971) "The problem of pile group-pile cap interaction", *Geotech*, 21 (2), 135-142.
- Das, A.K., and Deb, K., (2014) "Modelling of uniformly loaded circular raft resting on stone column – improved ground", *the Japanese geotechnical society soils and foundations*, 54(6), 1212-1224.
- Davis, E.H., and Poulos, H.G., (1972) "The analysis of pile-raft systems", *Aust. Geomech. J.*, G2 (1), 21-27 *Geotech.*, 50 (6), 689-698.
- El-Garhy, and Elsaywy, (2017) "Effect of different parameters on the behaviour of strip footing resting on weak soil improved by granular piles", *Int. Journal of Geo-Engineering*, 8:4, DOI: 10.1186/s40703-017-0042-2
- Elshazly, H.A., Hafez, D.H., and Mossaad, M.E., (2008) "Reliability of conventional settlement evaluation for circular foundations on stone columns", *Geotech Geol Eng*, 26(3), 323-334.
- Elwakil, A.Z., and Azzam, W.R., (2016) "Experimental and Numerical study of piled raft system", *Alexandria Engineering Journal*, 55, 547-560.
- Garg, V., Sharma, J. K., and Grover, K. D. S., (2018) "Stiffening Effect on Settlement Reduction for a Single Partially Stiffened Floating Granular Pile", *Journal of The Institution of Engineers (India)*, series A, DOI: 10.1007/s40030-018-0346-z.
- Garg, V., and Sharma, J.K., (2018) "Analysis and settlement of partially stiffened single and group of two floating granular piles", *Indian Geotechnical Journal*, 1-13. DOI: 10.1007/s40098-018-0321-7.
- Grover, K.S., Sharma, J.K., and Madhav, M.R., (2015) "Settlement analysis of single granular pile with stiffened top" *Int J Sci. Eng. Res.* 6(6), 61-75.
- Gupta, P. and Sharma, J.K., (2018) "Effect of Nonlinear Non-homogeneity of Floating Granular Pile and Soil on Settlement", *Journal of The Institution of Engineers (India)*, 1-11, series A
- Gupta, P. and Sharma, J.K., (2018) "Settlement analysis of non-homogeneous single granular pile", *Indian Geotech Journal*, 48(1), 92-101.
- Liang, F.Y., Chen, L.Z., and Shi, X.G., (2003) "Numerical analysis of composite piled raft with cushion subjected to vertical load" *computers and geotechnics* 30, 443-453.

- Madhav, M.R., Shahu, J.T., and Hayashi, S., (2000) "Analysis of soft ground-granular pile-granular mat system" *Computers and Geotechnics*, 27, 45-62.
- Madhav, M.R., Sharma, J. K. and Sivakumar, V. (2009), Settlement of and load distribution in a granular piled raft, *Geomechanics and Engineering*, Vol. 1, No. 1 (2009) 97-112.
- Madhav, M.R., Sharma, J.K. and Chandra, S. (2006), Analysis and settlement of a non-homogeneous granular pile, *Indian Geotechnical Journal*, 36(3), 249-271.
- Maheshwari, P., and Khatri, S., (2011) "A non-linear model for footings on granular bed-stone column reinforced earth beds", *Appl. Math. Modell.*, 35(6), 2790-2804.
- Maheshwari, P., and Khatri, S. (2010) "Non-linear response of footings on granular bed-stone column-reinforced poor soil", *Int. J. Geotech. Eng.*, 4(4), 435-443.
- Mindlin, R.D., (1936) "Force at a point in the interior of a semi-infinite solid", *Physics*, 7, 195-202.
- Balaam, N. P., and Booker, J. R., (1981) "Analysis of rigid rafts supported by granular piles", *Int. J. Numer. Anal. Meth. Geomech.*, 5, 379-403.
- Park, D., Park, D., and Lee, J., (2016) "Analyzing load response and load sharing behaviour of piled raft installed with driven piles in sands", *Computers and Geotechnics* 78, 62-71.
- Poulos, H.G., (1968) "The influence of rigid pile cap on the settlement behaviour of an axially loaded pile", *C.E. Trans. Inst. Engrs., Australia*, CE10 (2), 206-208.
- Randolph, M.F., (1983) "Design of piled raft foundations", *Proc. Int. Symp. On Recent Dev. In Lab. And Field Tests and Anal. Of Geotech. Problems*, Bangkok, 525-537.
- Sharma, J. K., Analysis and settlement of granular pile(s) - single, in group and with raft, A thesis submitted for the degree of Doctor of Philosophy to the Department of Civil Engineering, Indian Institute of Technology, Kanpur, India.
- Van Impe, W.F., and Madhav, M.R., (1992) "Analysis and settlement of dilating stone column reinforced soil", *Osterreichische Ing und Arch - Zeitschrift*, 137, 114-21.
- Wang, X., Zheng, J., and Yin, J., (2010) "On composite foundation with different vertical reinforcing elements under vertical loading: a physical model testing study" *Journal of Zhejiang University - Science A (Applied Physics & Engineering)* - 11(2), 80-87.
- Yamashita, K., and Yamada, T., (2009) "Settlement and load sharing of a piled raft with ground improvement on soft ground", *proceeding of 17th ICSMGE*, Vol.2, 1236-1239.
- Yamashita, K., Hamada, J., and Yamada, T., (2011) "Field measurements on piled rafts with grid-form deep mixing walls on soft ground", *Geotechnical Engineering Journal of the SEAGS & AGSSEA* Vol. 42, No. 2 ISSN 0046-5828

## 7. APPENDIX

### Granular Pile Displacements

Displacements of elements of GP are evaluated based on stress-strain relationship

$$\varepsilon_v = \frac{\sigma_v}{E_{gp}} \quad (1A)$$

Where  $\varepsilon_v$  and  $\sigma_v$  are the axial strains and the axial stress respectively on the element and  $E_{gp}$  is the deformation modulus of the granular pile.

#### (i) Relationship between Axial & Shear Stresses of GP

From the consideration of equilibrium, the total load, P, on GP is related to the shear stresses,  $\tau$ , and base pressure,  $p_b$ , as

$$P = \sum_{j=1}^n \frac{\tau_j \pi d L}{n} + p_b \frac{\pi d^2}{4} \quad (2A)$$

where 'n' is the total number of elements of GP. Considering the element 'i', (Figure 4 (c)) the axial forces on the top and bottom faces of the element are

$$P_{it} = P - \sum_{j=1}^{i-1} \frac{\tau_j \pi d L}{n} \quad (3A)$$

$$P_{ib} = P - \sum_{j=1}^i \frac{\tau_j \pi d L}{n}$$

Combining Eq.s (2A) & (3A)

$$P_{it} = \sum_{j=i}^n \frac{\tau_j \pi d L}{n} + p_b \frac{\pi d^2}{4} \quad (4A)$$

$$P_{ib} = \sum_{j=i+1}^n \frac{\tau_j \pi d L}{n} + p_b \frac{\pi d^2}{4}$$

The axial stresses on the top and bottom faces of the element 'i' are

$$\sigma_{it} = p_b + \sum_{j=i}^n \frac{n 4(L/d) \tau_j}{n} \quad (5A)$$

$$\sigma_{ib} = p_b + \sum_{j=i+1}^n \frac{4(L/d) \tau_j}{n}$$

The average axial stress,  $\sigma_{vi}$ , on the element, 'i' is

$$\sigma_{vi} = \frac{\sigma_{it} + \sigma_{ib}}{2} = p_b + \sum_{j=i+1}^n \frac{4(L/d) \tau_j}{n} + \frac{2(L/d) \tau_i}{n} \quad (6A)$$

The above equation relates shaft shear stresses to axial stresses of the elements and is expressed in matrix form as

$$\{\sigma_v\} = [A] \{\tau\} \quad (7A)$$

where  $\{\tau\}$  and  $\{\sigma_v\}$  are respectively columns vectors of shear stresses on shaft including normalized stress on the base and axial stresses of the elements, both of size (n+1). Matrix [A] is an upper triangular square matrix of size (n+1) which relates the axial and shear stresses as

$$[A] = \begin{bmatrix} \frac{2(L/d)}{n} & \frac{4(L/d)}{n} & \frac{4(L/d)}{n} & \frac{(L/d)}{n} & - & - & - & - & 1 \\ 0 & \frac{2(L/d)}{n} & \frac{4(L/d)}{n} & \frac{4(L/d)}{n} & - & - & - & - & 1 \\ 0 & 0 & \frac{2(L/d)}{n} & \frac{4(L/d)}{n} & - & - & - & - & 1 \\ - & - & - & - & 0 & \frac{2(L/d)}{n} & \frac{4(L/d)}{n} & 1 \\ - & - & - & - & - & 0 & \frac{2(L/d)}{n} & 1 \\ - & - & - & - & - & 0 & 0 & 1 \end{bmatrix} \quad (8A)$$

#### (ii) GP Displacements

Vertical displacements of granular pile are evaluated based on method given by Garg and Sharma (2018). The vertical displacements at each node of the elements of granular pile are evaluated starting from the top displacement of granular pile,  $\rho_1$  by progressing

downwards considering the strain of each element successively. The settlement of the first element of GP is

$$\rho_1^P = \frac{S_1^P}{d} = \rho_t - \varepsilon_{v1} \frac{\Delta z}{2d} \quad (9A)$$

where  $\varepsilon_{v1}$  is the axial strain of the first element of GP and  $\Delta z = (L/n)$ , is element length.  $S_1^P$  and  $\rho_1^P$  are the displacement and normalized displacements of the first node respectively. Thus, the displacement,  $\rho_i^P$ , of any element 'i' is obtained as

$$\rho_i^P = \rho_t - \sum_{j=1}^{i-1} \varepsilon_{vj} \frac{\Delta z}{d} - \varepsilon_{vi} \frac{\Delta z}{2d} \quad (10A)$$

where  $\varepsilon_{vi}$  and  $\varepsilon_{vj}$  are the axial strains of  $i^{\text{th}}$  and  $j^{\text{th}}$  elements respectively.

Due consideration is given to compatibility or continuity of displacement at the interface of stiffened and un-stiffened portions of GP. Considering the stiffening is carried out till the bottom of the  $m^{\text{th}}$  element from the top of the GP (Figure 4(a)), the displacement at the bottom of the  $m^{\text{th}}$  element or interface of stiffened and un-stiffened portion of GP is

$$\rho_{\text{interface}}^P = \rho_t - \sum_{j=1}^m \varepsilon_{vj} \frac{\Delta z}{d} \quad (11A)$$

In the above equation, for the calculation of  $\varepsilon_{vj}$ ,  $K_{\text{gp}}$  is taken for the stiffened portion. The displacement of the bottom of the  $m^{\text{th}}$  element of stiffened portion of GP is taken as the displacement of the top of the  $(m+1)^{\text{th}}$  element of un-stiffened portion of GP in order to satisfy the compatibility of displacements at the interface between the two parts. The displacement of center node of  $(m+1)^{\text{th}}$  element is evaluated as

$$\rho_{i=m+1}^P = \rho_t - \sum_{j=1}^m \varepsilon_{vj} \frac{\Delta z}{d} - \varepsilon_{vi} \frac{\Delta z}{2d} \quad (12A)$$

In the above equation, for the calculation of  $\varepsilon_{vj}$  and  $\varepsilon_{vi}$ , the following ratios,  $K_{\text{stgp}} = E_{\text{stgp}}/E_s$  and  $K_{\text{gp}} = E_{\text{gp}}/E_s$  are considered for the stiffened and un-stiffened portions respectively.

Displacement,  $\rho_i^P$ , of any general node  $i$  ( $> m$ ) below the interface can be evaluated as

$$\rho_i^P = \rho_t - \sum_{j=1}^m \varepsilon_{vj} \frac{\Delta z}{d} - \sum_{i=m+1}^{i-1} \varepsilon_{vi} \frac{\Delta z}{d} - \varepsilon_{vi} \frac{\Delta z}{2d} \quad (13A)$$

In the above equation, for the calculation of  $\varepsilon_{vj}$ ,  $K_{\text{stgp}} = E_{\text{stgp}}/E_s$  is taken for stiffened portion while for the calculation of  $\varepsilon_{vi}$ ,  $K_{\text{gp}} = E_{\text{gp}}/E_s$  is taken for the un-stiffened portion.

To evaluate the settlement of the base of granular pile, the strain at the base is

$$\varepsilon_b = -\frac{dS^P}{dz} = \frac{p_b}{E_{\text{gp}}} \quad (14A)$$

As suggested by Garg et al. (2018) using finite difference scheme with unequal intervals of spacing, the above equation is

$$\frac{4S_{n-1}^P - 36S_n^P + 32S_{n+1}^P}{12(\Delta z/d)} = -\frac{p_b}{E_{\text{gp}}} \quad (15A)$$

where  $S_{n-1}^P$ ,  $S_n^P$  and  $S_{n+1}^P$  are the displacements of elements  $n-1$ ,  $n$  and  $n+1$  respectively. Rewriting equation (15A) in the normalized form, one gets

$$4\rho_{n-1}^P - 36\rho_n^P + 32\rho_{n+1}^P = -\frac{p_b}{E_{\text{gp}}} \frac{12(L/d)}{n} \quad (16A)$$

Substituting for the values of  $\rho_{n-1}^P$  and  $\rho_n^P$  from Eq. (10A), and rearranging the terms, one gets

$$\rho_{n+1}^P = \rho_t - \sum_{j=1}^m \varepsilon_{vj} \frac{\Delta z}{d} - \sum_{j=m+1}^{j=(n-2)} \varepsilon_{vi} \frac{\Delta z}{d} - \frac{34}{32} \varepsilon_{v(n-1)} \frac{\Delta z}{d} - \frac{18}{32} \varepsilon_{vn} \frac{\Delta z}{d} - \frac{6}{32} \frac{(L/d)}{n} \frac{p_b}{E_s} \quad (17A)$$

In the above equation, for the calculation of  $\varepsilon_{vj}$ ,  $K_{\text{stgp}} = E_{\text{stgp}}/E_s$  is taken for stiffened portion while for calculation of  $\varepsilon_{vi}$ , and other  $\varepsilon_{vn}$ , and  $\varepsilon_{v(n-1)}$ ,  $K_{\text{gp}} = E_{\text{gp}}/E_s$  is taken for the un-stiffened portion.

Combining Eq.s (10A) & (17A), the vertical displacements of granular pile are

$$\{\rho^{PPV}\} = \rho_t \{1\} + [B] \left\{ \frac{\sigma_v}{E_s} \right\} \quad (18A)$$

$$[B] = \frac{(L/d)}{nK_{\text{gp}}} \begin{bmatrix} \frac{-0.5}{\mu} & 0 & 0 & 0 & - & - & - & 0 \\ \frac{-1}{\mu} & \frac{-0.5}{\mu} & 0 & 0 & - & - & - & 0 \\ \frac{-1}{\mu} & \frac{-1}{\mu} & \frac{-0.5}{\mu} & 0 & - & - & - & - \\ \frac{-1}{\mu} & \frac{-1}{\mu} & \frac{-1}{\mu} & 0 & - & - & - & - \\ - & - & - & - & - & - & - & - \\ \frac{-1}{\mu} & \frac{-1}{\mu} & \frac{-1}{\mu} & - & - & - & -0.5 & 0 \\ \frac{-1}{\mu} & \frac{-1}{\mu} & \frac{-1}{\mu} & - & - & - & \frac{34}{32} & \frac{18}{32} & \frac{6}{32} \end{bmatrix} \quad (19A)$$

where  $[B]$  is lower triangular matrices of sizes  $(n+1) \times (n+1)$ .

Here in matrix  $[B]$   $K_{\text{stgp}}$  is replace by  $\mu$ ,  $K_{\text{gp}}$  for top elements of GP for the effect of stiffening upto depth  $\lambda L/d$ .

Using the elemental shear and axial stresses (Equation (9A)), the vertical displacements of GP nodes in terms of interface shear stresses are

$$\{\rho^{PPV}\} = \rho_t \{1\} + [C] \left\{ \frac{\tau}{E_s} \right\} \quad (20A)$$

where  $[C]$  is a square matrix of size,  $(n+1) = [B] [A]$ .